The DØ Detector Upgrade and Physics Program

John Ellison

Department of Physics, University of California
Riverside, CA 92521-0413, USA

for the DØ Collaboration

Abstract

The DØ detector at Fermilab is in the final stages of an extensive upgrade. It is designed to meet the demands imposed by high luminosity Tevatron running planned to begin March 2001. The design and performance of the detector subsystems are described and a brief outline of the physics potential is presented.

1 Introduction

The future physics program at Fermilab will be greatly enhanced by the Tevatron upgrade which will result in an increase in luminosity and allow datasets of 100 times those collected in Run I. This upgrade will be accompanied by a decrease in the bunch crossing time from the Run I value of 3.5 μs to 396 ns and finally to 132 ns as the number of bunches is increased in stages.

To take full advantage of the new physics opportunities and to contend with the much higher radiation environment and shorter bunch crossing times, an extensive upgrade of the DØ detector was undertaken, and is now in its final stages.

The upgrade consists of the addition of a cosmic ray scintillator shield and bunch tagging system, the replacement of the front end electronics for the calorimeter and the muon system, the upgrade of the muon detection system, the replacement of the tracking system for both the central and forward regions, the addition of preshower detectors, and improvements to the trigger and data acquisition systems. Figure 1 shows an elevation view of the upgraded detector.

2 Tracking

The tracking system (Fig. 2) consists of an inner silicon microstrip tracker (SMT), surrounded by a central scintillating fiber tracker (CFT). These systems are contained within the bore of a 2T superconducting solenoid, which is surrounded by a scintillator preshower detector.

The upgraded tracking system has been designed to meet several goals: momentum measurement by the introduction of a solenoidal field; good electron identification and e/π rejection; tracking over a large range in pseudorapidity ($\eta \approx \pm 3$); secondary vertex measurement for identification of b-jets from Higgs and top decays and for b-physics; first level tracking trigger; fast detector response to enable operation with a bunch crossing time of 132 ns; and radiation hardness.

2.1 Silicon Microstrip Tracker

The silicon tracking system is based on 50 μm pitch silicon microstrip detectors providing a spatial resolution of approximately 10 μm in $r\phi$. The high resolution is important to obtain good momentum measurement and vertex reconstruction. The detector consists of a system of barrels and interleaved disks designed to provide good coverage out to $\eta \approx 3$ for all tracks emerging from the interaction region, which is distributed along the beam direction with $\sigma_z \approx 25$ cm.

The barrel has 6 sections, each 12 cm long and containing 4 layers. The first and third layers of the inner 4 barrels are constructed of double-sided 90°-stereo detectors with axial strips and orthogonal z strips at pitches of 50 μm and 153.5 μm respectively. The outer two barrels use single-sided detectors with 50 μm pitch axial strips in layers 1 and 3. In all six barrels the second and fourth layers are made from double-sided detectors with axial and 2° stereo strips at 50 μm and 62.5 μm pitch respectively . The combination of small-angle and large-angle stereo provides good pattern recognition and allows good

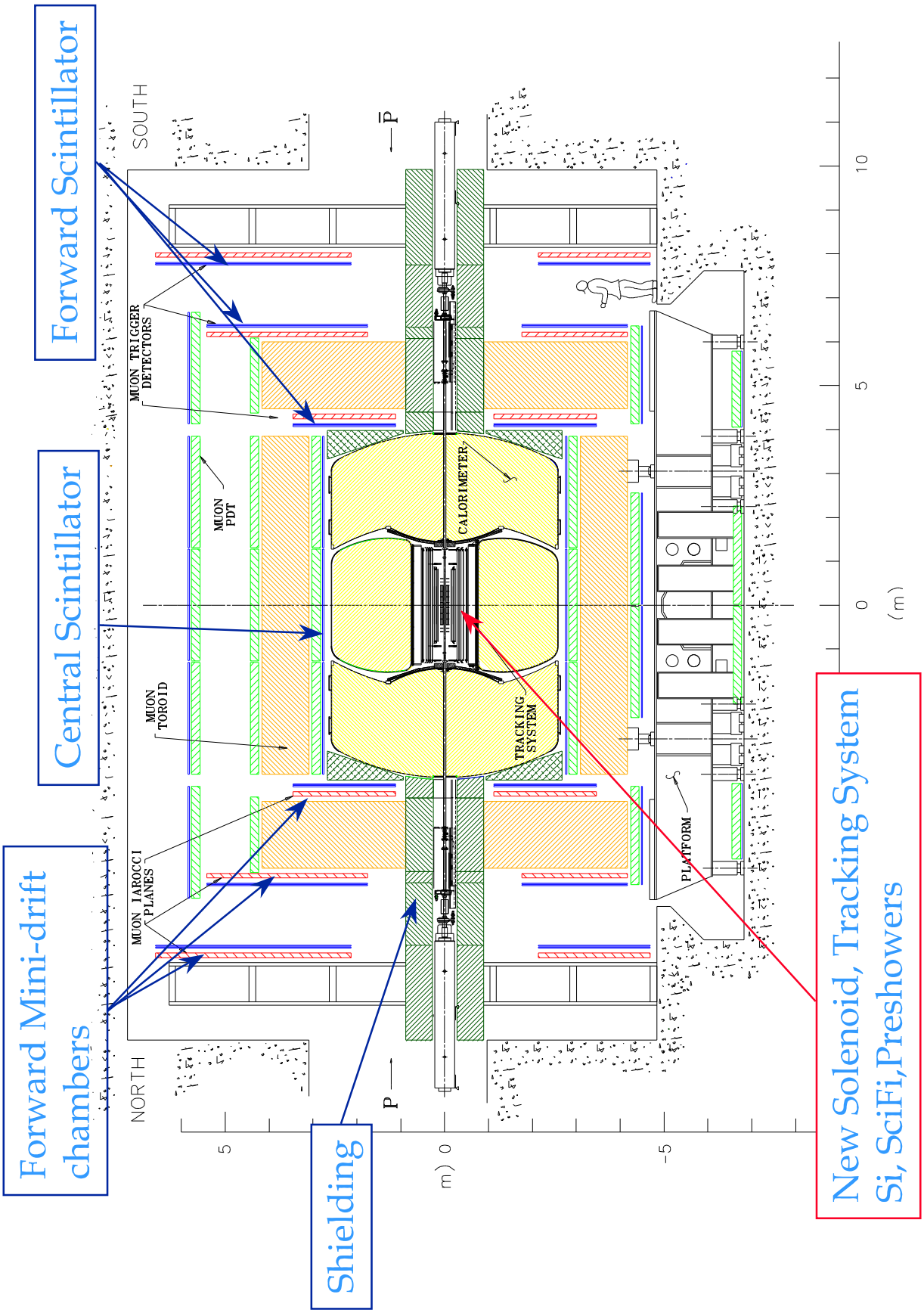

Figure 1: Elevation view of the upgraded DØ detector for Run II.

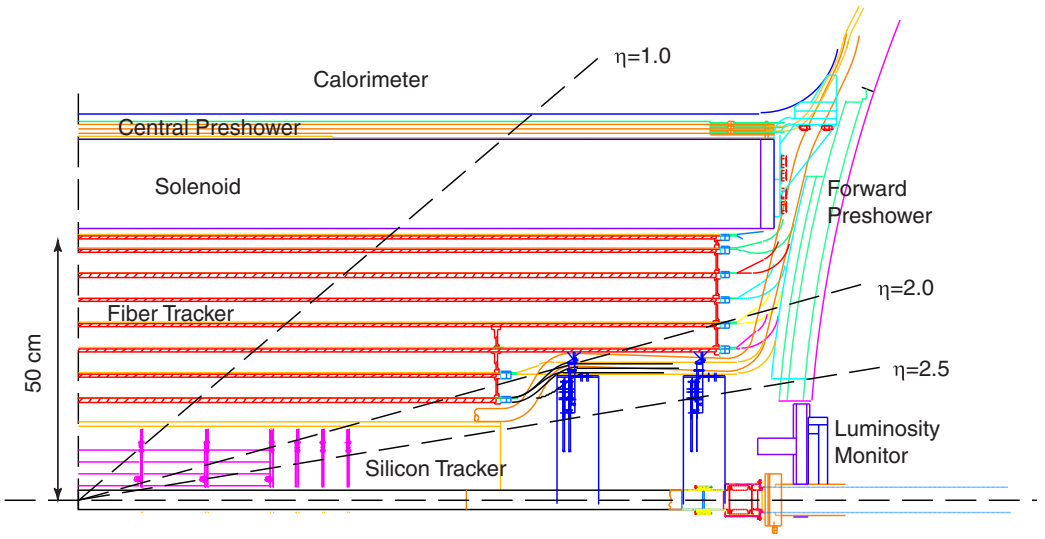

Figure 2: $r-z$ view of the DØ tracking system.

separation of primary vertices in multiple interaction events. The expected hit position resolution in $r\phi$ is 10 μm, and for the 90°-stereo detectors it is about 40 μm in z.

The forward disk system consists of double-sided detectors with $\pm 15°$ stereo strips at 50 μm and 62.5 μm pitch. The H-disks, which cover the high-η regions, are constructed from two back-to-back single-sided detectors with $\pm 7°$ stereo strips at 80 μm pitch

The silicon detectors are ac-coupled – each strip has an integrated coupling capacitor and polysilicon bias resistor. The front end CMOS readout chip (SVX IIe) [1] contains 128 channels, each channel comprising a double-correlated sampling amplifier, a 32-cell analog pipeline, and an analog-to-digital converter. The chip also contains sparse readout circuitry to limit the total readout time. The SVX IIe chips are mounted on a kapton high density circuit which is glued to the surface of the silicon detector. The detectors are mounted on beryllium bulkheads which serve as a support and provide cooling via water flow through beryllium tubes integrated into the bulkheads. The silicon tracker has a total of 793,000 channels. Figure 3 show a cross sectional view in the $r-\phi$ plane of a barrel section.

A silicon track trigger preprocessor is being built which will allow use of SMT information at Level 2. This will add the capability for triggering on tracks displaced from the primary vertex, as well as sharpen the p_T threshold of the Level 2 track trigger and of the electron and jet triggers at Level 3.

2.2 Scintillating Fiber Tracker

The outer tracking in the central region is based on scintillating fiber technology with visible light photon counter (VLPC) readout [2]. The CFT consists of 8 layers, each containing 2 fiber doublets in a zu or zv configuration (z = axial fibers and $u, v = \pm 3°$ stereo fibers). Each doublet consists of two layers of 830 μm diameter fibers with 870 μm spacing, offset by half the fiber spacing. The fibers are supported on carbon fiber support cylinders. This configuration provides very good efficiency and pattern recognition and results in a position resolution of $\approx$ 100 μm in $r\phi$.

The fibers are up to 2.5 m long and the light is piped out by clear fibers of length 7-11 m to the VLPC's situated in a cryostat outside the tracking volume, which is maintained at 9°K. The VLPC's are solid state devices with a pixel size of 1 mm, matched to the fiber diameter. The fast risetime, high gain and excellent quantum efficiency of these devices makes them ideally suited to this application.

The CFT has a total of about 77,000 channels. Since this technology is rather novel we have done extensive testing. This includes the characterization of thousands of channels of VLPC's and the setup of a cosmic ray test stand with fully instrumented fibers. The measured photoelectron yield, a critical measure of the system performance, was found to be 8.5 photoelectrons per fiber, with operation such that 99.5% of the thermal noise was below a threshold of one photoelectron. This is well above the requirement of

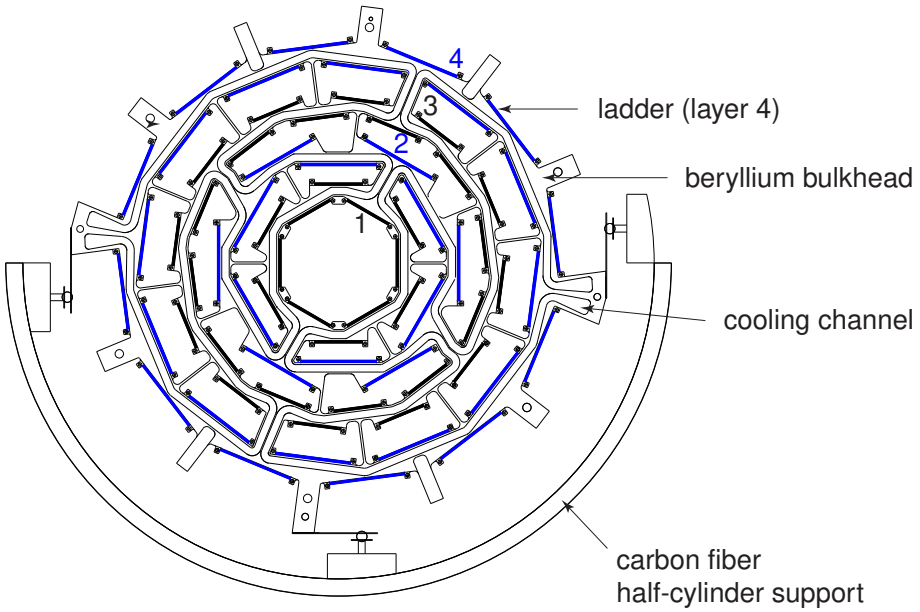

Figure 3: Cross sectional $r\phi$ view of an SMT barrel.

2.5 photoelectrons needed for fully efficient tracking based on detailed GEANT simulations. The tracking efficiency measured in the cosmic ray stand is $\epsilon > 99.9\%$. Figure 4 shows the pulse height distribution for cosmic ray muons. Also shown is a histogram of the fitted track residuals, from which a fiber doublet resolution of 92 μm is determined.

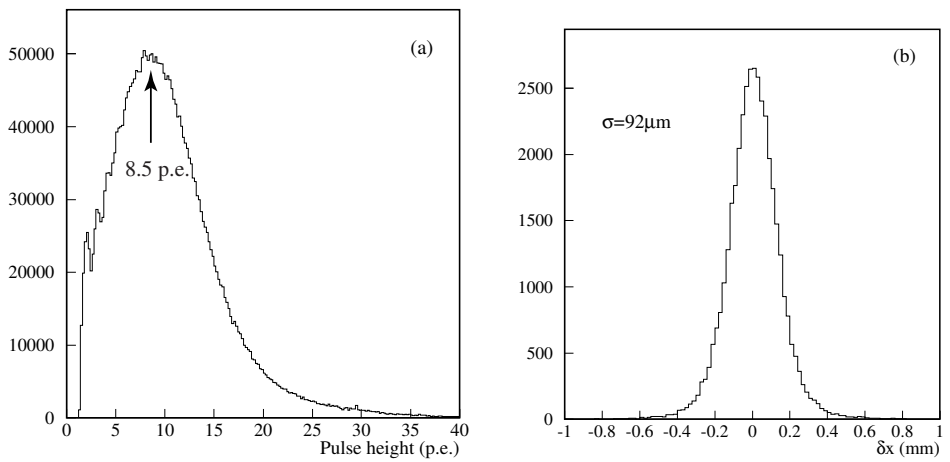

Figure 4: CFT cosmic ray test stand results: (a) photoelectron yield per fiber; (b) distribution of doublet residuals from fitted tracks.

2.3 Superconducting Solenoid

The superconducting solenoid is 2.73 m in length and 1.42 m in diameter and provides a 2 T magnetic field, allowing charged particle momentum measurement. The solenoid is wound with two layers of mulifiliamentary Cu:NbTi wire strands, stabilized with aluminum. Eighteen strands are used in each conductor. To ensure good field uniformity, the current density is larger at the ends of the coil. The thickness of the magnet system is approximately one radiation length.

3 Preshower detectors

The central and forward preshower detectors (CPS and FPS) provide fast energy and position measurements for the electron trigger and offline electron identification. The preradiator consists of 5.5 mm lead in the CPS and 11 mm of lead in the FPS (see Fig. 5).

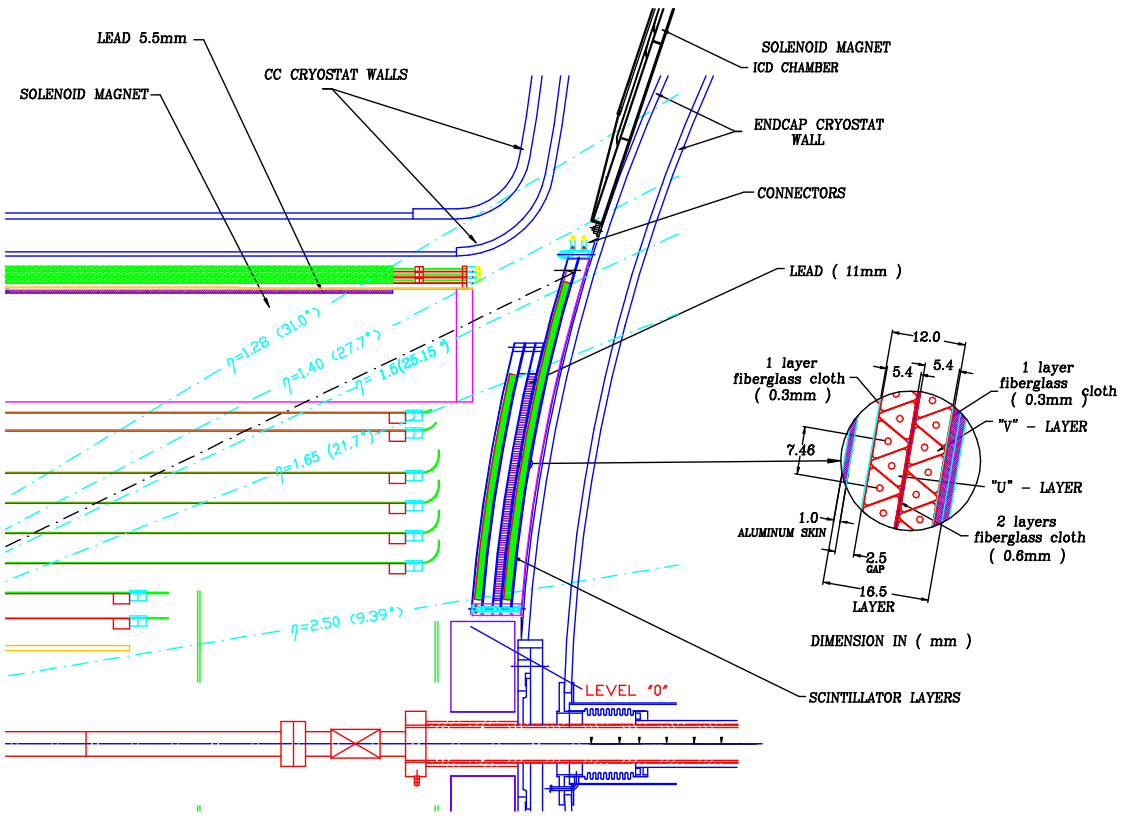

Figure 5: The central and forward preshower detectors, with a detail of the FPS construction.

The CPS detector consists of three concentric cylindrical layers of interleaved triangular scintillator strips. The three layers are arranged in an xuv geometry (x = axial, $uv = \pm$ stereo angle of approximately 23°). Wavelength shifting fibers are used to pipe the light out to a VLPC readout system.

The position resolution for 10 GeV electrons is estimated from Monte Carlo to be < 1.4 mm. Cosmic ray tests have been performed to study the light yield and resolution [3]. Figure 6 shows some results. The light yield is shown in Fig. 6(a) together with the simulated yield for a cosmic ray muon passing through a "singlet" (i.e. a single layer of triangular strips) and a "doublet" (two layers of strips). The readout fiber in this setup was 11 m in length. Figure 6(b) shows the fitted track residuals. The measured doublet position resolution for cosmic ray muons is 550 μm.

The forward preshower detector is constructed from two uv layers of triangular strips. A detail of the design in shown in Fig. 5.

4 Muon Detectors

The Run I forward muon drift chambers would suffer from excessive aging effects in the Run II environment, and therefore a complete replacement of the forward muon systems has been undertaken. In the central region, the existing proportional drift tubes are retained, but with the faster gas Ar-CH_4-CF_4 (80%:10%:10%) resulting in a maximum drift time of 500 ns. The contribution to the hit position uncertainty due to diffusion is about 375 μm (compared with 300 μm for the slower Run I gas). However,

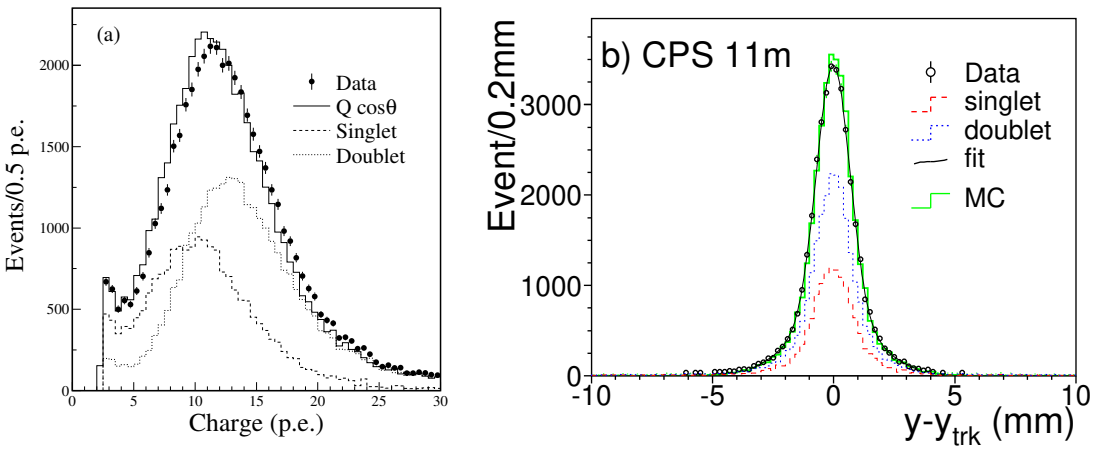

Figure 6: Preshower detector cosmic ray muon tests: (a) light yield (p.e. = photoelectrons); (b) fitted track residuals.

the decreased number of proton-antiproton beam crossings within the drift time ($\simeq 2$ for 396 ns operation and $\simeq 4$ for 132 ns operations) results in reduced occupancy and improved triggering.

The front end electronics has also been replaced to ensure deadtimeless operation. To augment the central PDT's a layer of scintillation counters has been added, situated just outside the calorimeter. The counters are segmented in z (9 counters) and ϕ (80 counters), and the position measurement is used to match to tracks in the the CFT and in the muon PDT's. The scintillator time resolution is 1.6 ns, which enables out-of-time backgrounds to be rejected.

The Run II forward muon system consists of three layers of mini drift tubes and three layers of scintillation counters covering $1 < |\eta| < 2$. The mini drift tubes consist of 1 cm $\times$ 1 cm cells produced in 8-cell extrusions. They are operated in proportional mode using a fast gas (90% CF_4 - 10% CH_4) and have a drift time of 60 ns.

Non-muon backgrounds in the muon detectors are reduced by shielding situated around the beampipe in the forward regions (see Fig. 1). These backgrounds are due to scattered p and $\bar{p}$ fragments interacting with the calorimeter and low-beta quadrupole magnets, and beam halo interactions. The shielding consists of 39 cm of iron (which acts as a hadron and electromagnetic absorber), 15 cm of polyethylene (which has a high hydrogen content and absorbs neutrons), and 15 cm of lead (which absorbs gamma rays).

5 Trigger and Data Acquisition

The DØ trigger and DAQ systems have been completely restructured to handle the shorter bunch spacing and new detector subsystems in Run II. The level 1 and 2 triggers utilize information from the calorimeter, preshower detectors, central fiber tracker, and muon detectors. The level 1 trigger reduces the event rate from 7.5 MHz to 10 kHz and has a latency of 4 μsec. The trigger information is refined at level 2 using calorimeter clustering and detailed matching of objects from different subdetectors. The level 2 trigger has an accept rate of 1 kHz and a latency of 100 μsec. Level 3, consisting of an array of PC processors, partially reconstructs event data within 50 msec to reduce the rate to 50 Hz. Events are then written to tape.

6 Detector Performance

New capabilities of the DØ detector include:

- Lower muon trigger thresholds with no prescale (single muon trigger threshold $p_T > 7$ GeV, dimuon trigger threshold $p_T > 2$ GeV)

- Reduced muon backgrounds and trigger rates due to the additional shielding
- Calorimeter performance comparable to that in Run I, with the new capability to calibrate using the tracking system momentum measurement
- Increased trigger capabilities (more than an order of magnitude over Run I)
- Improved electron identification from the addition of the preshower detectors: an additional factor of 3-5 rejection in the forward region over using the calorimeter alone

As well as these benefits the new tracking system allows momentum measurement and secondary vertex tagging. The momentum resolution of the tracking system is shown in Fig. 7. At $\eta = 0$ the resolution is approximately $\delta p_T/p_T = 17\%$ for $p_T = 100$ GeV. With this resolution the upgrade tracking will enable E/p matching for electron identification, improve the muon momentum resolution, provide charge sign determination for charged particles and help in calorimeter calibration.

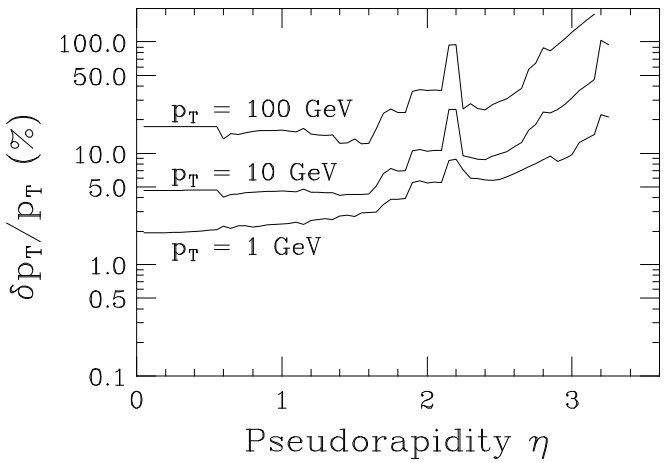

Figure 7: Transverse momentum resolution vs. psuedorapidity.

The tracking system will also be used to tag displaced secondary vertices, especially important for the Higgs search, and for $t\bar{t}$ physics and b-physics. Fig. 8 shows the resolution of the 2-dimensional $r\phi$ impact parameter as a function of pseudorapidity. The resolution is less than 20 μm for tracks with $p_T < 1$ GeV over the approximate range $\eta \leq 2$, which is the region of interest for tagging b-jets from top decays. Based on a parameterized Monte Carlo simulations of PYTHIA $p\bar{p} \to WH \to \ell\nu\ b\bar{b}$ events and ISAJET $p\bar{p} \to t\bar{t} \to \ell\nu +$ jets events, we expect a b-tagging efficiency of $\simeq 55\%$, decreasing at low b-jet p_T, as shown in Fig. 9.

7 Physics Program – Selected Highlights

One of the most important goals of Run II is the search for the Higgs boson. Assuming that the correct explanation of electroweak symmetry breaking is the Higgs mechanism, fits to electroweak data show that the Higgs mass is less than 170 GeV at the 95% confidence level. Direct searches at LEP rule out a Higgs mass below 113 GeV, while recent indications from LEP suggest the possibility of a Higgs signal at $m_H \simeq 115$ GeV [4]. This is precisely the Higgs mass range accessible at the Tevatron, provided sufficient integrated luminosity is achieved. Recently, there has been much attention paid to this, and detailed studies have been performed as part of the Tevatron Run II Workshop [5]. This is described in the talk by V. Kuznetsov at this conference [6]. The expected sensitivity is summarized in Fig. 10. Note that a Higgs boson can be excluded up to a mass of about 180 GeV and discovery of the Higgs is possible over some of this range.

Another primary goal of the DØ upgrade physics program is the study of the top quark. Since the CM energy is expected to increase from 1.8 TeV to $\approx$2 TeV, the $t\bar{t}$ production cross section will increase

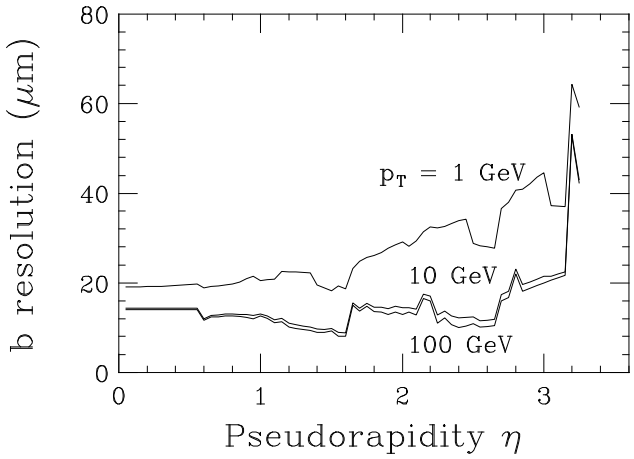

Figure 8: 2d impact parameter resolution in the $r\phi$ plane vs. pseudorapidity.

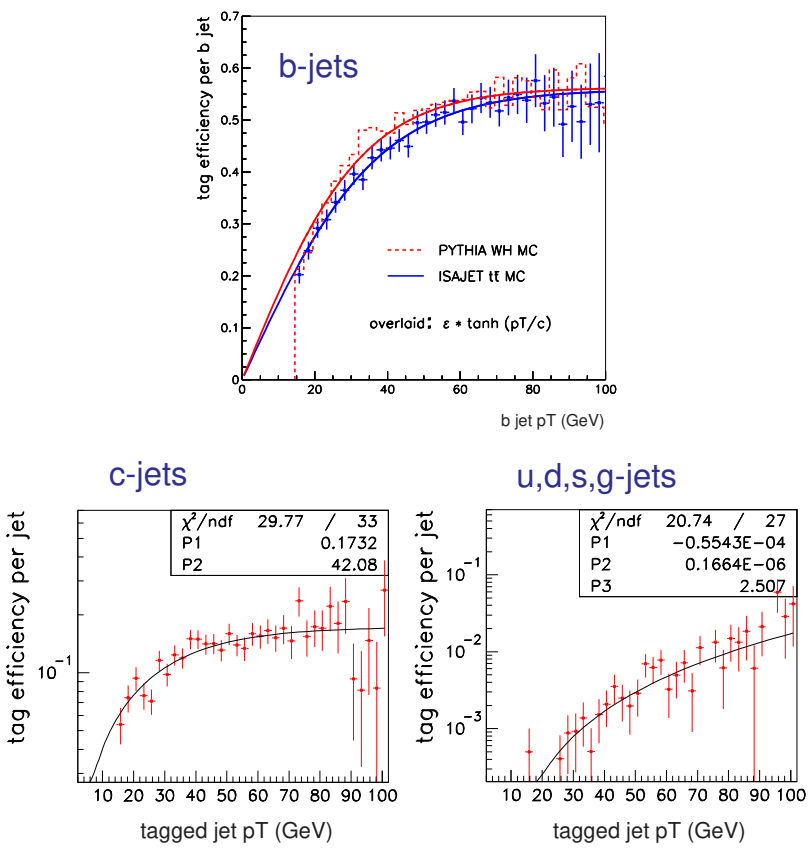

Figure 9: Efficiency for tagging b-jets, c-jets, and light-quark/gluon jets as a function of jet p_T from parameterized simulations of WH and $t\bar{t}$ events.

by about 38% (the production is dominated by $q\bar{q} \to t\bar{t}$.) For single top production the increase will be about 22% for the s-channel ($q\bar{q} \to t\bar{b}$), and about 44% for the W-gluon fusion process ($qg \to qt\bar{b}$). The expected uncertainty in the top quark mass measurement is $\delta m_t \simeq 3$ GeV. The $t\bar{t}$ production cross section is expected to be measured with about 9% accuracy. Production and decay properties will be studied in detail. For example, $t\bar{t}$ spin correlations, which are transmitted to the decay products since the top decays before hadronization, can be observed with an uncertainty on the spin correlation coefficient

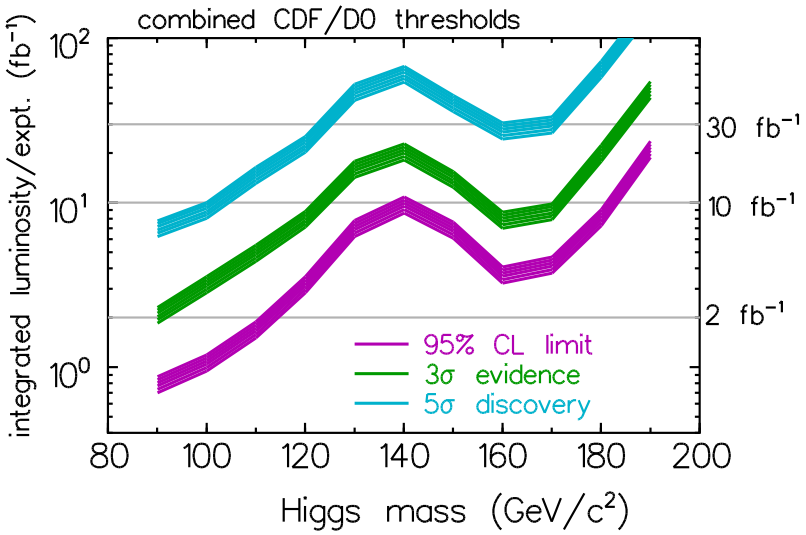

Figure 10: Integrated luminosity required as a function of Higgs mass for a 95% C.L. exclusion, 3σ evidence and 5σ discovery.

κ of $\delta\kappa \simeq 0.4$. Studies of the kinematic properties in $t\bar{t}$ events will also be sensitive to physics beyond the standard model. For example, one can search for resonances in the invariant $t\bar{t}$ mass spectrum, such as a Z' predicted by topcolor assisted technicolor.

In Run II we will also be able to observe single top production. Since this process involves production of a top quark at the Wtb vertex, it is sensitive to magnitude of the CKM matrix element V_{tb}. A measurement of $|V_{tb}|$ with accuracy better than $\pm 15\%$ will be possible in Run II. Furthermore, deviations from the $V-A$ nature of the Wtb coupling can be probed.

An important goal of electroweak physics in Run II is the measurement of the W boson mass. With an integrated luminosity of 2 fb^{-1} per experiment the level of statistical precision will be of order 10 MeV and systematic errors in the measurement and model will dominate. An uncertainty of approximately $\delta m_W = 30$ MeV from the combination of CDF and DØ measurements seems achievable [7].

The search for new phenomena will be another important part of the physics program in Run II. I will not attempt to enumerate the possibilities here, but will mention only some highlights of the expectations for Supersymmetry signals. Fig. 11 shows the potential for observing gaugino pair production in the trilepton decay modes $p\bar{p} \to \tilde{\chi}_1^{\pm}\tilde{\chi}_1^{\mp}, \tilde{\chi}_1^{\pm}\tilde{\chi}_2^0 \to 3\ell + X$ plotted for the minimal supergravity framework in the $(m_{1/2}, m_0)$ plane, where $m_{1/2}$ and m_0 are the universal scalar and fermion masses at the GUT scale. This process can probe $m_{1/2}$ up to ~ 250 GeV for favorable values of the model parameters, which corresponds to a gluino mass of ~ 600 GeV. For large tanβ, stau decays of the gauginos will be dominant, resulting in tau lepton signatures. The upgraded DØ tracking system will improve the tau identification capabilities, thus aiding in this search.

Supersymmetric squark/gluino production in the jets + $\not\!\!E_T$ channel is expected to probe masses up to about 350-375 GeV for 2 fb^{-1}. The sensitivity to stop and sbottom squarks depends on their decay modes: if $\tilde{t} \to b\tilde{\chi}_1^{\pm}$ or $\tilde{t} \to b\ell\tilde{\nu}$, masses up to 250 GeV can be probed.

Interesting possibilities for utilizing the new capabilities of the upgraded detector exist in several scenarios of SUSY. For example, in gauge-mediated SUSY breaking the gravitino $\tilde{G}$ is the LSP. If the $\tilde{\chi}_1^0$ is the NLSP, then $\tilde{\chi}_1^0 \to \gamma\tilde{G}$ and one can search for gaugino pair production using the $\gamma\gamma + \not\!\!E_T$ final state. The excellent $\not\!\!E_T$ resolution in DØ can be used and, if the decay has a long lifetime so that the photons are displaced from the primary vertex, the calorimeter and preshower detector can be used to project the photon back to the beamline with an uncertainty of $\simeq 2$ cm. Alternatively, if the $\tilde{\tau}$ is the NLSP then $\tilde{\tau} \to \tau\tilde{G}$, and the signature is τ's + $\not\!\!E_T$. If the $\tilde{\tau}$ is long-lived, large impact parameter τ's or heavily ionizing $\tilde{\tau}$'s may then be important, which can be identified from large impact parameter tracks or high dE/dx in the SMT.

For an integrated luminosity of 2 fb^{-1} at the Tevatron approximately 10^{11} b-quark pairs will be

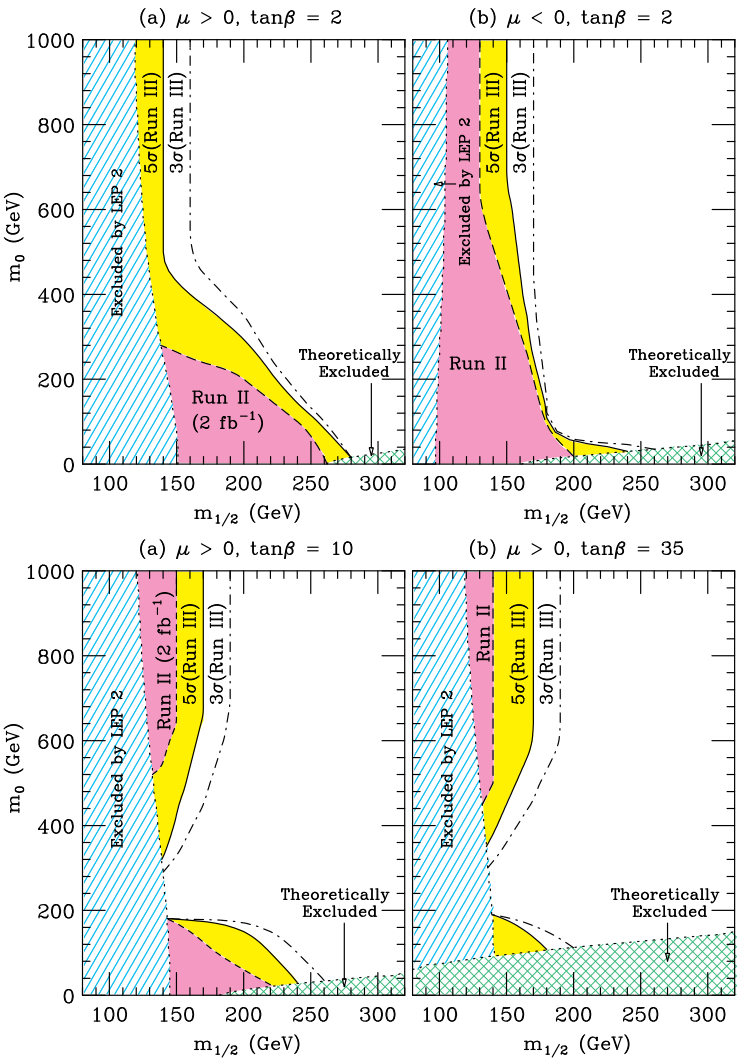

Figure 11: Contours of 99% C.L. observation in Run II (2 fb^{-1}) for gaugino pair production in the trilepton decay modes plotted in the $(m_{1/2}, m_0)$ plane: (a) $\tan\beta = 2, \mu > 0$; (b) $\tan\beta = 2, \mu < 0$; (c) $\tan\beta = 10, \mu > 0$; (d) $\tan\beta = 35, \mu > 0$. Also shown are the contours for a 3σ observation and 5σ discovery in Run III (30 fb^{-1}). From Ref. [8].

produced. Therefore, a wide range of b-physics studies will be possible. These include b-quark cross sections, rare B decays, B_s mixing and CP violation in the $B - \overline{B^0}$ system. In contrast to high p_T physics, B mesons are produced at relatively high η and low p_T. Therefore, tracking and vertexing out to $\eta \approx 3$ is important for b-physics studies. Simulations indicate that B_s mixing could be detected for values of the mixing parameter x_s up to 30 for DØ and 60 for CDF, and that CP violation could be accessible with an error on $\sin(2\beta)$ of about 0.04 for each experiment with 2 fb^{-1} of data. For more details see Ref. [6].

Acknowledgments

I would like to thank the QFTHEP2000 organizers for arranging a stimulating workshop and for their warm hospitality.

References

[1] T. Zimmerman, et al., IEEE Trans. Nucl. Sci. **42** (1995) 803.

[2] M.D. Petroff and M.G. Staplebroek, IEEE Trans. Nucl. Sci., **3 6**, No. 1 (1989) 158; M.D. Petroff and M. Attac, IEEE Trans. Nucl. Sci., **36**, No. 1 (1989) 163.

[3] P. Baringer et al., (DØ Collaboration), " Cosmic Ray Tests of the DØ Preshower Detector", submitted to Nucl. Instrum. Meth. A. hep-ex/0007026.

[4] The LEP Higgs Working group, "Standard Model Higgs Boson at LEP: Results with the 2000 Data, Request for Running in 2001".
`http://lephiggs.web.cern.ch/LEPHIGGS/papers/doc_nov3_2000.ps`

[5] M. Carena et al., Report of the Tevatron Higgs Working Group, hep-ph/0010338.

[6] V. Kuznetsov, these proceedings.

[7] R. Brock et al., Report of the Working Group on Precision Measurements, hep-ex/0011009.

[8] S. Abel et al., Report of the SUGRA Working Group for Run II of the Tevatron, hep-ph/0003154.